Inorg. Chem. **2006**, *45*, 10207–10214

Inorganic Chemistry Article

New Layered Uranium Phosphate Fluorides: Syntheses, Structures, Characterizations, and Ion-Exchange Properties of $A(UO_2)F(HPO_4)\cdot xH_2O$ ($A = Cs^+$, Rb^+, K^+; $x = 0$–1)

Kang Min Ok,[†] Jaewook Baek,[‡] P. Shiv Halasyamani,[‡] and Dermot O'Hare*,[†]

Chemistry Research Laboratory, University of Oxford, Oxford, OX1 3TA, United Kingdom, and Department of Chemistry, University of Houston, Houston, Texas 77204-5003

Received July 28, 2006

Single crystals of three new layered uranium phosphate fluorides, $A(UO_2)F(HPO_4)\cdot xH_2O$ ($A = Cs^+$, Rb^+, and K^+; $x = 0$–1) have been synthesized by hydrothermal reactions using UO_3, H_3PO_4, HF, and corresponding alkali metal halides as reagents. Although all three new materials have layered structures, each of them contains different structural motifs within the layer. While $Cs(UO_2)F(HPO_4)\cdot 0.5H_2O$ and $Rb(UO_2)F(HPO_4)$ reveal noncentrosymmetric crystal structures, $K(UO_2)F(HPO_4)\cdot H_2O$ crystallizes in a centrosymmetric space group. In addition, the ion-exchanged phases for all three materials are highly crystalline. Crystal data: $Cs(UO_2)F(HPO_4)\cdot 0.5H_2O$, orthorhombic, space group $Pca2_1$ (No. 29), with $a = 25.656(5)$ Å, $b = 6.0394(12)$ Å, $c = 9.2072(18)$ Å, and $Z = 4$; $Rb(UO_2)F(HPO_4)$, orthorhombic, space group $Cmc2_1$ (No. 36), with $a = 17.719(4)$ Å, $b = 6.8771(14)$ Å, $c = 12.139(2)$ Å, and $Z = 8$; $K(UO_2)F(HPO_4)\cdot H_2O$, monoclinic, $P2_1/n$ (No. 14), with $a = 6.7885(14)$ Å, $b = 8.7024(17)$ Å, $c = 12.020(2)$ Å, $\beta = 94.09(3)°$, and $Z = 4$.

Introduction

Hydrothermal reaction techniques for the synthesis of new materials containing various structural motifs have been well-established.[1−8] In this synthetic method, both acids and bases are often used as mineralizers to increase the solubility of the reagents.[9,10] Moreover, either organic or inorganic structure-directing agents play a profound role to influence a variety of framework formations and subsequent physical properties.[1,2,11] It has proven possible to synthesize a vast range of layered or framework materials, by careful control of the synthesis conditions as well as introducing proper electronic and steric template materials. Among many structurally versatile cations, U^{6+} has been used widely owing to its rich structural diversity with a higher coordination sphere; excellent ability to accommodate different polyhedral units; and potential applications such as catalysis, ion-exchange, and intercalation properties.[11−14] To date, one of the most studied uranyl material fields is uranyl phosphate compounds, in which the phosphate group shares its corner or edge with a uranyl group and exhibits the full range of structural diversity, from zero-dimensional molecular compounds to three-dimensional microporous frameworks.[15−32]

* Author to whom correspondence should be addressed. Phone: 44-1865-285130. Fax: 44-1865-272690. E-mail: dermot.ohare@chem.ox.ac.uk.
[†] University of Oxford.
[‡] University of Houston.

(1) Breck, D. W. *Zeolite Molecule Sieves: Structure, Chemistry and Use*; Wiley and Sons: London, 1974.
(2) Barrer, R. M. *Hydrothermal Chemistry of Zeolites*; Academic Press: London, 1982.
(3) Clearfield, A. *Chem. Rev.* **1988**, *88*, 125.
(4) Davis, M. E.; Lobo, R. F. *Chem. Mater.* **1992**, *4*, 756.
(5) Venuto, P. B. *Microporous Mater.* **1994**, *2*, 297.
(6) Feng, P.; Bu, X.; Stucky, G. D. *Nature (London)* **1997**, *388*, 735.
(7) Cheetham, A. K.; Ferey, G.; Loiseau, T. *Angew. Chem., Int. Ed.* **1999**, *38*, 3268.
(8) Natarajan, S.; Neeraj, S.; Choudhury, A.; Rao, C. N. R. *Inorg. Chem.* **2000**, *39*, 1426.
(9) Laudise, R. A. *J. Am. Chem. Soc.* **1958**, *81*, 562.
(10) Laudise, R. A.; Ballman, A. A. *J. Am. Chem. Soc.* **1958**, *80*, 2655.
(11) Szostak, R. *Molecular Sieves: Principles of Synthesis and Identification*; Reinhold: New York, 1989.
(12) Weiss, A.; Hartl, K.; Hofmann, U. *Z. Naturforsch., B: Chem. Sci.* **1957**, *12*, 669.
(13) Pekarek, V.; Vesely, V. J. *Inorg. Nucl. Chem.* **1965**, *27*, 1151.
(14) Grohol, D.; Blinn, E. L. *Inorg. Chem.* **1997**, *36*, 3422.
(15) Piret, P.; Piret-Meunier, J.; Declercq, J. P. *Acta Crystallogr., Sect. B* **1979**, *35*, 1880.
(16) Fitch, A. N.; Fender, B. E. F. *Acta Crystallogr., Sect. C* **1983**, *39*, 162.
(17) Piret, P.; Piret-Meunier, J.; Deliens, M. *Eur. J. Mineral.* **1990**, *2*, 399.
(18) Cole, M.; Fitch, A. N.; Prince, E. *J. Mater. Chem.* **1993**, *3*, 519.
(19) Benard, P.; Louer, D.; Dacheux, N.; Brandel, V.; Genet, M. *Chem. Mater.* **1994**, *6*, 1049.
(20) Guesdon, A.; Raveau, B. *Chem. Mater.* **1998**, *10*, 3471.
(21) Francis, R. J.; Drewitt, M. J.; Halasyamani, P. S.; Ranganathachar, C.; O'Hare, D.; Cleggb, W.; Teat, S. J. *Chem. Commun.* **1998**, 279.

10.1021/ic061420d CCC: $33.50
Published on Web 11/15/2006

Meanwhile, the fluoride anion from hydrofluoric acid has also been used in the hydrothermal synthesis reactions as a mineralizer.[33−39] Larger amounts of F^- ions often lead to it being incorporated into the reaction product, which increases the possibility for new and varied structure types, with fluoride providing an extra coordination mode for the U^{6+} centers. Interestingly, although a number of natural and synthetic uranium phosphate materials have been reported, uranium phosphate fluoride materials are rarely observed. In fact, to the best of our knowledge, synthetic $[N_2C_6H_{14}]_2$-$[(UO_2)_6(H_2O)_2F_2(PO_4)_2(HPO_4)_4]\cdot 4H_2O$[40] and the mineral uranospathite $Al_{1-x}\delta_x[(UO_2)(PO_4)]_2(H_2O)_{20+3x}F_{1-3x}$[41] are the only known uranium phosphate fluoride materials. Here, we report the synthesis, structures, characterizations, and ion-exchange properties of three new series of uranium phosphate fluoride materials, $Cs(UO_2)F(HPO_4)\cdot 0.5H_2O$, $Rb(UO_2)F(HPO_4)$, and $K(UO_2)F(HPO_4)\cdot H_2O$. These compounds are designated as LUPF-1, LUPF-2, and LUPF-3, respectively (LUPF = layered uranium phosphate fluoride). Although each of these compounds reveals similar stoichiometry with layered geometry, all crystallize in different space groups with dissimilar structural morphologies. Thus, the effect of templating cations on the structural variations is also discussed.

Experimental Section

Caution: *Although all uranium materials used in these experiments were depleted, extra care and good laboratory practice should always be used when handling uranium-containing materials. HF is toxic and corrosive.*

Reagents. UO_3 (99.8%, Strem), CsCl (99%, Aldrich), RbF (99.8%, Aldrich), KCl (99.0%, Aldrich), HF [40% (aq), BDH], and H_3PO_4 [85% (aq), BDH] were used as received.

Syntheses. For $Cs(UO_2)F(HPO_4)\cdot 0.5H_2O$ (LUPF-1), 0.572 g (2.00×10^{-3} mol) of UO_3 and 0.337 g (4.00×10^{-3} mol) of CsCl were combined with 0.8 g of aqueous H_3PO_4 (85%), 0.1 g of aqueous HF (40%), and 6 mL of deionized water. For $Rb(UO_2)F(HPO_4)$ (LUPF-2), 0.572 g (2.00×10^{-3} mol) of UO_3 and 0.379 g (3.63×10^{-3} mol) of RbF were combined with 0.8 g of aqueous H_3PO_4 (85%), 0.1 g of aqueous HF (40%), and 6 mL of deionized water. For $K(UO_2)F(HPO_4)\cdot H_2O$ (LUPF-3), 0.572 g (2.00×10^{-3} mol) of UO_3 and 0.274 g (3.68×10^{-3} mol) of KCl were combined with 0.8 g of aqueous H_3PO_4 (85%), 0.1 g of aqueous HF (40%), and 6 mL of deionized water.

The respective solutions were placed in 23-mL Teflon-lined autoclaves that were subsequently sealed. The autoclaves were heated to 200 °C, held for 48 h, and cooled slowly at a rate of 3 °C h^{-1} to 150 °C, and then at 6 °C h^{-1} to room temperature. After cooling to room temperature, the autoclaves were opened and the products were recovered by filtration and washed with water. For LUPF-1, LUPF-2, and LUPF-3, yellow plate crystals, the only product from the reaction, were recovered in 93%, 76%, and 84% yields, respectively, based on UO_3. Powder X-ray diffraction (XRD) patterns on the synthesized phases are in good agreement with the generated pattern from the single-crystal data (see the Supporting Information). Elemental microanalysis for LUPF-1 obsd (calcd): U, 45.21% (45.26%); P, 5.86% (5.89%); Cs, 25.21% (25.22%). LUPF-2 obsd (calcd): U, 50.18% (50.59%); P, 6.59% (6.58%); Rb, 18.24% (18.17%). LUPF-3 obsd (calcd): U, 53.47% (53.96%); P, 6.91% (7.02%); K, 8.73% (8.84%).

Crystallographic Determination. The structures of LUPF-1, LUPF-2, and LUPF-3 were determined by standard crystallographic methods. Data were collected using an Enraf Nonius FR 590 Kappa CCD diffractometer with graphite monochromated Mo Kα radiation. Crystals were mounted on a glass fiber using N-paratone oil and cooled in situ using an Oxford Cryostream 600 Series to 150 K for data collection. Frames were collected, indexed, and processed using Denzo SMN and the files scaled together using HKL GUI within Denzo SMN.[42] The heavy atom positions were determined using SIR97.[43] All other sites were located from Fourier difference maps. All heavy atoms were refined using anisotropic thermal parameters using full-matrix least-squares procedures on F_o^2 with $I > 3\sigma(I)$. All calculations were performed using the WinGX 98 crystallographic software package.[44] Crystallographic data and selected bond distances for LUPF-1, LUPF-2, and LUPF-3 are given in Tables 1−4.

Powder X-ray Diffraction. Powder XRD patterns were recorded on a PANalytical X'Pert Pro diffractometer using Cu Kα radiation at room temperature with 40 kV and 40 mA. Samples were mounted on aluminum plates and scanned in the 2θ range 5−60° with a step size of 0.02° and a step time of 1 s.

Infrared and Raman Spectroscopy. Infrared spectra were recorded on a Bio-Rad FTS 6000 FT-IR spectrometer in the 400−4000 cm^{-1} range, with the sample intimately contacted by a diamond as an attenuated total reflectance crystal. Raman spectra were recorded on a Jobin Yvon spectrometer (Labram 1B) equipped with a microscope, through a 50-fold magnification objective (Olympus company). A 40 mW argon-ion laser (514 nm) was used. The 1800 L/mm grating provides a resolution starting from 1.5 cm^{-1} at 200 cm^{-1} up to 1.0 cm^{-1} at 3600 cm^{-1}. The abscissa was calibrated with the 520.7 cm^{-1} peak of a silicon standard, and the sharp Raman shifts are accurate within the limits of the resolution.

Nonlinear Optical Measurements. Powder second harmonic generation (SHG) measurements for the noncentrosymmetric

(22) Burns, P. C. *Am. Mineral.* **2000**, *85*, 801.
(23) Danis, J. A.; Runde, W. H.; Scott, B.; Fettinger, J.; Eichhorn, B. *Chem. Commun.* **2001**, 2378.
(24) Doran, M.; Walker, S. M.; O'Hare, D. *Chem. Commun.* **2001**, 1988.
(25) Locock, A. J.; Burns, P. C. *J. Solid State Chem.* **2002**, *163*, 275.
(26) Locock, A. J.; Burns, P. C. *J. Solid State Chem.* **2002**, *167*, 226.
(27) Locock, A. J.; Burns, P. C. *Can. Mineral.* **2003**, *41*, 91.
(28) Locock, A. J.; Burns, P. C.; Duke, M. J. M.; Flynn, T. M. *Can. Mineral.* **2004**, *42*, 973.
(29) Burns, P. C.; Alexopoulos, C. M.; Hotchkiss, P. J.; Locock, A. J. *Inorg. Chem.* **2004**, *43*, 1816−1818.
(30) Locock, A. J.; Burns, P. C.; Flynn, T. M. *Am. Mineral.* **2005**, *90*, 240.
(31) Shvareva, T. Y.; Sullens, T. A.; Shehee, T. C.; Albrecht-Schmitt, T. E. *Inorg. Chem.* **2005**, *44*, 300.
(32) Shvareva, T. Y.; Albrecht-Schmitt, T. E. *Inorg. Chem.* **2006**, *45*, 1900.
(33) Estermann, M.; McCusker, L. B.; Baerlocher, C.; Merrouche, A.; Kessler, H. *Nature (London)* **1991**, *352*, 320.
(34) Ferey, G. *J. Fluorine Chem.* **1995**, *72*, 187.
(35) Chen, C. Y.; Finger, L. W.; Medrud, R. C.; Crozier, P. A.; Chan, I. Y.; Harris, T. V.; Zones, S. I. *Chem. Commun.* **1997**, 1779.
(36) Bull, I.; Villaescusa, L. A.; Teat, S. J.; Camblor, M. A.; Wright, P. A.; Lightfoot, P.; Morris, R. E. *J. Am. Chem. Soc.* **2000**, *122*, 7128.
(37) Corma, A.; Diaz-Cabanas, M. J.; Martinez-Triguero, J.; Rey, F.; Rius, J. *Nature (London)* **2002**, *418*, 514.
(38) Doran, M. B.; Cockbain, B. E.; Norquist, A. J.; O'Hare, D. *Dalton Trans.* **2004**, 3810.
(39) Ok, K. M.; Doran, M. B.; O'Hare, D. *J. Mater. Chem.* **2006**, In Press.
(40) Doran, M. B.; Stuart, C. L.; Norquist, A. J.; O'Hare, D. *Chem. Mater.* **2004**, *16*, 565.
(41) Locock, A. J.; Kinman, W. S.; Burns, P. C. *Can. Mineral.* **2005**, *43*, 989.
(42) Otwinowski, Z. *Data Collection and Processing*; Daresbury Laboratory: Warrington, U. K., 1993.
(43) Cascarano, G.; Giacovazzo, C.; Guagliardi, A. *J. Appl. Crystallogr.* **1993**, *26*, 343.
(44) Farrugia, L. J. *J. Appl. Crystallogr.* **1999**, *32*, 837.

Table 1. Crystallographic Data for $Cs(UO_2)F(HPO_4)\cdot 0.5H_2O$ (LUPF-1), $Rb(UO_2)F(HPO_4)$ (LUPF-2), and $K(UO_2)F(HPO_4)\cdot H_2O$ (LUPF-3)

formula	$Cs_2(UO_2)_2F_2(HPO_4)_2\cdot H_2O$	$Rb(UO_2)F(HPO_4)$	$K(UO_2)F(HPO_4)\cdot H_2O$
fw	1053.82	470.47	442.12
space group	$Pca2_1$ (No. 29)	$Cmc2_1$ (No. 36)	$P2_1/n$ (No. 14)
a (Å)	25.656(5)	17.719(4)	6.7885(14)
b (Å)	6.0394(12)	6.8771(14)	8.7024(17)
c (Å)	9.2072(18)	12.139(2)	12.020(2)
β (deg)	90	90	94.09(3)
V (Å^3)	1426.6(5)	1479.2(5)	708.3(2)
Z	4	8	4
T (°C)	150.0(2)	150.0(2)	150.0(2)
λ (Å)	0.710 73	0.710 73	0.710 73
ρ_{calcd} (g cm^{-3})	4.907	4.306	4.146
μ (mm^{-1})	28.012	28.704	23.743
$R(F)^a$	0.0491	0.0584	0.0411
$R_w(F_o^2)^b$	0.1201	0.1325	0.0999

^{a} $R(F) = \sum||F_o| - |F_c||/\sum|F_o|$. ^{b} $R_w(F_o^2) = [\sum w(F_o^2 - F_c^2)^2/\sum w(F_o^2)^2]^{1/2}$.

Table 2. Selected Bond Distances (Å) for LUPF-1

U(1)−O(1)	1.801(15)	U(2)−O(6)	1.795(14)	P(1)−O(3)	1.526(14)
U(1)−O(2)	1.783(16)	U(2)−O(7)	1.781(14)	P(1)−O(5)	1.511(14)
U(1)−O(3)	2.318(13)	U(2)−O(8)	2.294(16)	P(1)−O(10)	1.526(14)
U(1)−O(4)	2.324(15)	U(2)−O(9)	2.350(15)	P(1)−O(11)	1.574(16)
U(1)−O(5)	2.343(14)	U(2)−O(10)	2.355(13)	P(2)−O(4)	1.501(16)
U(1)−F(1)	2.334(13)	U(2)−F(1)	2.388(13)	P(2)−O(8)	1.527(16)
U(1)−F(2)	2.347(13)	U(2)−F(2)	2.391(14)	P(2)−O(9)	1.518(16)
				P(2)−O(12)	1.611(15)

Table 3. Selected Bond Distances (Å) for LUPF-2

U(1)−O(1)	1.873(18)	P(1)−O(3)	1.54(2)
U(1)−O(2)	1.667(17)	P(1)−O(4)	1.527(16)
U(1)−O(3)	2.339(19)	P(1)−O(5)	1.528(18)
U(1)−O(4)	2.279(15)	P(1)−O(6)	1.55(2)
U(1)−O(5)	2.363(17)		
U(1)−F(1)	2.348(9)		
U(1)−F(2)	2.357(11)		

Table 4. Selected Bond Distances (Å) for LUPF-3

U(1)−O(1)	2.308(7)	P(1)−O(1)	1.525(7)
U(1)−O(2)	2.308(6)	P(1)−O(2)	1.524(7)
U(1)−O(3)	2.360(7)	P(1)−O(3)	1.521(7)
U(1)−O(4)	1.775(7)	P(1)−O(6)	1.603(7)
U(1)−O(5)	1.783(7)		
U(1)−F(1)	2.365(6)		
U(1)−F(1)	2.382(5)		

materials were performed on a modified Kurtz-NLO system with 1064 nm light.[45] A detailed description of the equipment and methodology used has been published elsewhere.[46,47] Crystalline SiO_2 was used to make relevant SHG intensity. No index matching fluid was used in the experiments.

Thermogravimetric Analysis. Thermogravimetric analyses were carried out on a TGA 2950 thermogravimetric analyzer (TA Instruments). The samples were contained within platinum crucibles and heated at a rate of 10 °C min^{-1} from room temperature to 800 °C in static air.

Ion-Exchange Experiments. Ion-exchange reactions were performed by stirring ca. 200 mg of polycrystalline LUPF-1, LUPF-2, and LUPF-3 in 10 mL of 1 M aqueous solution of the following metal salts: LiCl, $NaNO_3$, KNO_3, and RbF. The reactions were performed at room temperature for 24 h and then at 50 °C for 48 h. The ion-exchanged products were recovered by filtration, washed with excess H_2O, and dried in air for 1 day. The extent of the ion exchange was investigated by inductively coupled plasma (ICP) analysis.

Elemental Analysis. The compositions of the reported materials and the ion-exchanged solids were determined by ICP analysis using a Thermo Jarrell Ash Scan 16 instrument.

Results and Discussions

LUPF-1 has a layered structure consisting of seven-coordinated UO_5F_2 and four-coordinated $PO_3(OH)$ units connected by P−O−U and U−F−U bonds (see Figure 1). There are two crystallographically unique U^{6+} cations in the LUPF-1 structure. Both U^{6+} cations are bonded to five oxygen atoms and two fluorine atoms, resulting in distorted pentagonal bipyramidal environments. While the axial U═O distances for each UO_5F_2 unit range from 1.781(14) to 1.801(15) Å, the equatorial U−O distances range from 2.294(16) to 2.355(13) Å. The U−F distances range from 2.334(13) to 2.391(14) Å. The two unique P^{5+} cations are connected to four oxygen atoms. One of the oxygen atoms bonded to the P^{5+} cation is an OH group; thus, the four-coordinate asymmetric $PO_3(OH)$ tetrahedral moiety is observed around the P^{5+} cation. In fact, the lengths of the P−O bonds range from 1.501(16) to 1.527(16) Å. However, longer distances of 1.574(16) and 1.611(15) Å are observed from the P−OH bonds. To identify the positions of H^+, the hydrogen bonds in the structure were analyzed. We observe that hydrogen bonds occur from O(11) and O(12) to the oxygen atoms of the occluded water molecule [O(11)···O(w1) 2.718(18) Å, O(12)···O(w1) 2.609(18) Å; see Figure 2]. Moreover, bond valence calculations on these terminal oxygen sites reveal very similar values of 1.30 and 1.37 for O(11) and O(12), respectively, which are also consistent with our model. Finally, the IR spectrum confirms the presence of a P−OH group (see spectroscopic studies). The two U^{6+} cations share their edges through F(1) and F(2) atoms

(45) Kurtz, S. K.; Perry, T. T. *J. Appl. Phys.* **1968**, *39*, 3798.
(46) Ok, K. M.; Bhuvanesh, N. S. P.; Halasyamani, P. S. *J. Solid State Chem.* **2001**, *161*, 57.
(47) Porter, Y.; Ok, K. M.; Bhuvanesh, N. S. P.; Halasyamani, P. S. *Chem. Mater.* **2001**, *13*, 1910.

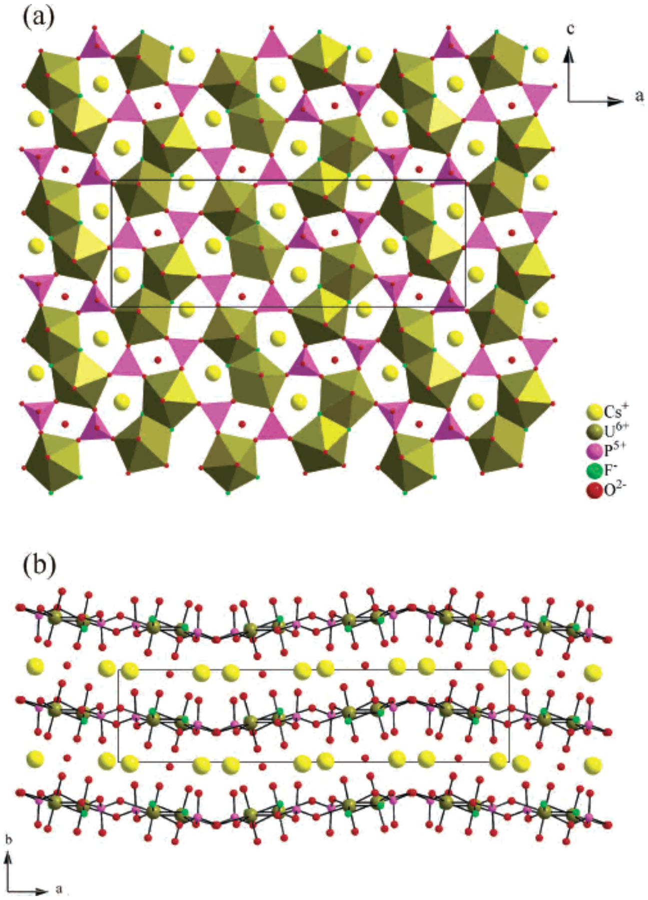

Figure 1. (a) Polyhedral representation of the uranium phosphate layer in the *ac* plane and (b) ball-and-stick representation in the *ab* plane of the LUPF-1. Note the $[(UO_2)O_3]_2F_2$ dimers and HPO_4 tetrahedra generate four- and five-membered rings within the layer.

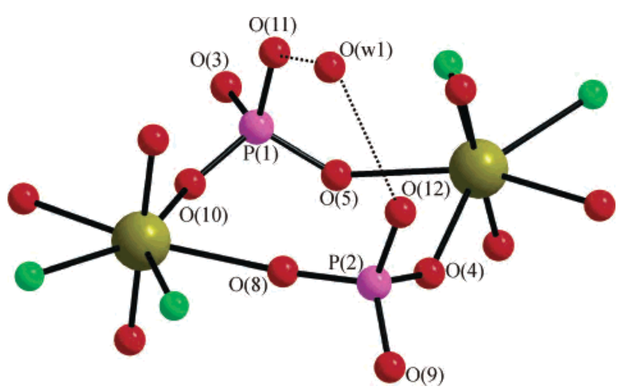

Figure 2. Hydrogen-bonding interactions between the water molecule and hydroxyl group in LUPF-1.

resulting in the formation of $[(UO_2)O_3]_2F_2$ dimers. These dimers are further connected by HPO_4 tetrahedra within the layer to generate four- and five-membered rings (see Figure 1a). A 2_1 screw axis is observed along the polar *c* axis. In connectivity terms, the entire layer can be described as a $\{[UO_{2/1}O_{3/2}F_{2/2}]^{2-}[PO_{3/2}(OH)]^{+}\}^{-}$ sheet. The anionic layers are separated by Cs^+ cations and occluded H_2O molecules. Bond valence calculations[48−50] on LUPF-1 resulted in values 5.78−5.87 and 4.97−5.01 for U^{6+} and P^{5+}, respectively.

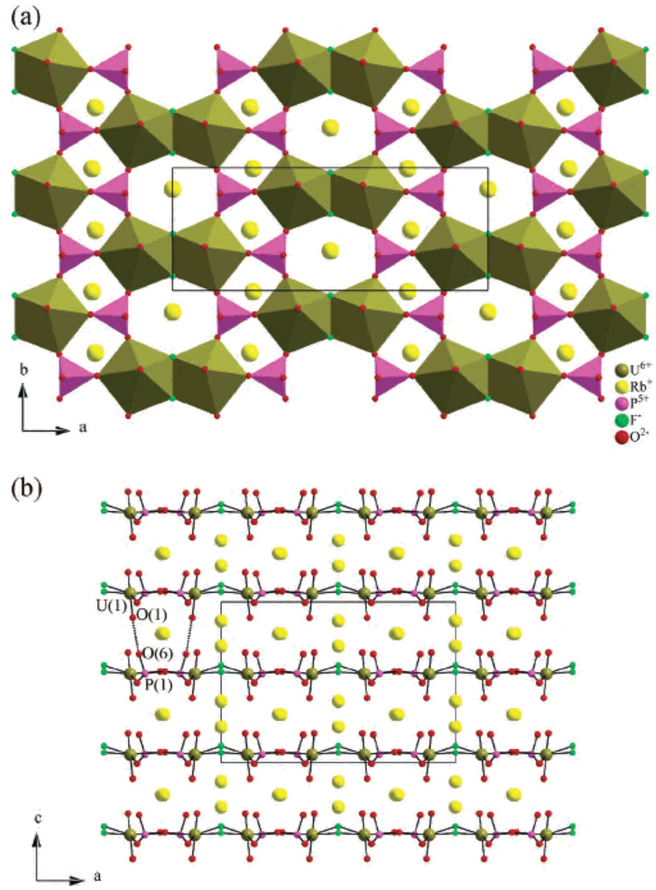

Figure 3. Polyhedral and ball-and-stick representations for the uranium phosphate layer of the LUPF-2 (a) in the *ab* plane and (b) in the *ac* plane. Note the $[(UO_2)O_3]_2F_2$ dimers and HPO_4 tetrahedra generate four- and six-membered rings within the layer. Hydrogen-bonding interactions between O(1) and O(6) have all the HPO_4 tetrahedra align along the [001] direction.

LUPF-2 exhibits a two-dimensional layered structure, with UO_5F_2 polyhedra linked to asymmetric HPO_4 tetrahedra through oxygen atoms (see Figure 3). In examining the thermal ellipsoid for LUPF-2, we determined that the Rb(1) atom could be split over two sites, Rb(1) and Rb(2), and fractional occupancy must occur in the Rb(3) to retain charge balance. In doing so, fractional occupancies of 0.549(18), 0.531(18), and 0.544(7) were refined for Rb(1), Rb(2), and Rb(3), respectively. Each U^{6+} cation is bonded to five oxygen atoms and two fluorine atoms, in a distorted pentagonal bipyramidal environment with the axial U═O distances ranging from 1.667(17) to 1.873(18) Å, the equatorial U−O distances ranging from 2.279(15) to 2.363(17) Å, and the U−F distances ranging from 2.348(9) to 2.357(11) Å. One of the axial uranyl U═O bond distances in LUPF-2 [1.873(18) Å] seems longer than those of previously reported uranyl bonds. As we discuss later, the elongation of the uranyl bond might be due to strong hydrogen bonds between O(1) in the uranyl group and O(6) in the HPO_4 group (see Figure 3b). All three of the equatorial oxygen atoms are further bonded to P^{5+} cations. The distances for the P−O bonds range from 1.527(16) to 1.55(2) Å. Similar to LUPF-1, one of the oxygen atoms bonded to the P^{5+} cation in LUPF-2 is an −OH group.

(48) Brown, I. D.; Altermatt, D. *Acta Crystallogr., Sect. B* **1985**, *41*, 244.
(49) Brese, N. E.; O'Keeffe, M. *Acta Crystallogr., Sect. B* **1991**, *47*, 192.
(50) Burns, P. C.; Ewing, R. C.; Hawthorne, F. C. *Can. Mineral.* **1997**, *35*, 1551.

We observe that hydrogen bonds occur from the terminal oxygen atom, O(6), to the axial uranyl oxygen atom [O(1)···O(6) 2.808(1) Å]. Bond valence calculations [1.34 for O(6)] and the IR spectrum confirm the presence of the P−OH group (see spectroscopic studies). Two U^{6+} cations are sharing their edges through fluorine atoms and are forming $[(UO_2)O_3]_2F_2$ dimers that are similarly observed in LUPF-1. However, unlike LUPF-1, the connectivity of the $[(UO_2)O_3]_2F_2$ dimers and HPO_4 tetrahedra within each layer generates four- and six-membered rings along the [001] direction (see Figure 3). This similar layer topology has been observed in the naturally occurring mineral johannite and some synthetic uranyl compounds.[51−53] However, all of the tetrahedral units surrounding the $[(UO_2)O_3]_2F_2$ dimers in the johannite-like materials are coordinated on both sides, that is, above and below, which make the structure centrosymmetric. The main difference occurring in LUPF-2 is that all of the asymmetric HPO_4 tetrahedra align and point along the [001] direction and make the structure noncentrosymmetric, which is the most interesting structural characteristic of LUPF-2 (see Figure 3). This asymmetric alignment of HPO_4 tetrahedra might be due to the hydrogen-bonding interactions between the axial uranyl oxygen atom, O(1), and the terminal oxygen atom, O(6) (see Figure 3b). In connectivity terms, the structure can be written as $\{[UO_{2/1}O_{3/2}F_{2/2}]^{2-}[PO_{3/2}(OH)]^{+}\}^{-}$, with the charge neutrality maintained by the Rb^+ cation. Rb^+ cations reside between the layers. Bond valence calculations[48−50] on LUPF-2 resulted in values of 6.06 and 4.98 for U^{6+} and P^{5+}, respectively.

LUPF-3 crystallizes in centrosymmetric space group $P2_1/n$ and also has a two-dimensional layered crystal structure consisting of UO_5F_2 pentagonal bipyramids linked to HPO_4 tetrahedra through oxygen atoms (see Figure 4). The axial U═O distances are ranging from 1.775(7) to 1.783(7) Å, the equatorial U−O distances are ranging from 2.308(7) to 2.360(7) Å, and the U−F distances are ranging from 2.365(6) to 2.382(5) Å. While in LUPF-1 and LUPF-2, the UO_5F_2 pentagonal bipyramids share their edges through fluorine atoms to produce $[(UO_2)O_3]_2F_2$ dimers, the UO_5F_2 pentagonal bipyramids in LUPF-3 share their corners through fluorine atoms and form infinite chains along the [010] direction. The distances for the P−O bonds range from 1.521(7) to 1.603(7) Å. Similar to Cs and Rb phases, an −OH group is also observed from one of the oxygen atoms bonded to the P^{5+} cation in LUPF-3. We observe that strong hydrogen bonds occur from the terminal oxygen atom in the HPO_4 group, O(6), to the oxygen atom in the water molecule [O(6)···O(w1) 2.655(17) Å] (see Figure 5). Similar to LUPF-1 and LUPF-2, bond valence calculations [1.31 for O(6)] and the IR spectrum support the presence of a P−OH group (see spectroscopic studies). The UO_5F_2 infinite chains are further interconnected to HPO_4 tetrahedra through oxygen atoms and produce a sheet that consists of three- and five-membered rings (see Figure 4). This similar layer topology has been

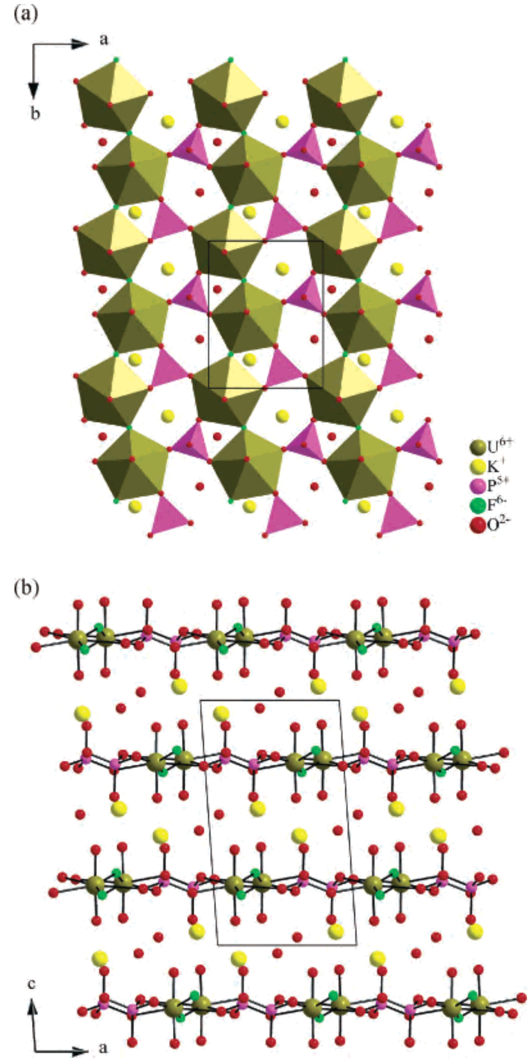

Figure 4. (a) Polyhedral representation of the uranium phosphate layer in the *ab* plane and (b) ball-and-stick representation in the *ac* plane of the LUPF-3. Note the UO_5F_2 infinite chains and HPO_4 tetrahedra generate three- and five-membered rings within the layer.

observed from $[NH_4][UO_2F(SeO_4)]\cdot H_2O$[54] and $[N_2C_3H_{12}][UO_2F(SO_4)]_2\cdot H_2O$.[53] In connectivity terms, the structure maybe be written as $\{[UO_{2/1}O_{3/2}F_{2/2}]^{2-}[PO_{3/2}(OH)]^{+}\}^{-}$, with the charge neutrality maintained by the K^+ cation. Between the layers are the K^+ cations and occluded H_2O molecules. Bond valence calculations[48−50] on LUPF-3 resulted in values of 5.90 and 4.90 for U^{6+} and P^{5+}, respectively.

Although LUPF-1, LUPF-2, and LUPF-3 are stoichiometrically similar, the structures of the materials are different. All three phases share a two-dimensional layered structure containing UO_5F_2 and HPO_4 units, and the alkali metal cations reside between the layers. However, while LUPF-1 and LUPF-2 crystallize in the noncentrosymmetric space groups $Pca2_1$ and $Cmc2_1$, respectively, LUPF-3 crystallizes in the centrosymmetric space group $P2_1/n$. Obviously, the size of alkali metal cations plays a role in determining the centricity of the materials. It has been known that larger cations tend to adopt an asymmetric coordination environ-

(51) Mereite, K. *Tschermaks Mineral. Petrogr. Mitt.* **1982**, *30*, 49.
(52) Halasyamani, P. S.; Francis, R. J.; Walker, S. M.; O'Hare, D. *Inorg. Chem.* **1999**, *38*, 271.
(53) Doran, M. B.; Cockbain, B. E.; O'Hare, D. *Dalton Trans.* **2005**, 1774.
(54) Blatov, V. A.; Serezhkina, L. B.; Serezhkin, V. N.; Trunov, V. K. *Zh. Neorg. Khim.* **1989**, *34*, 162.

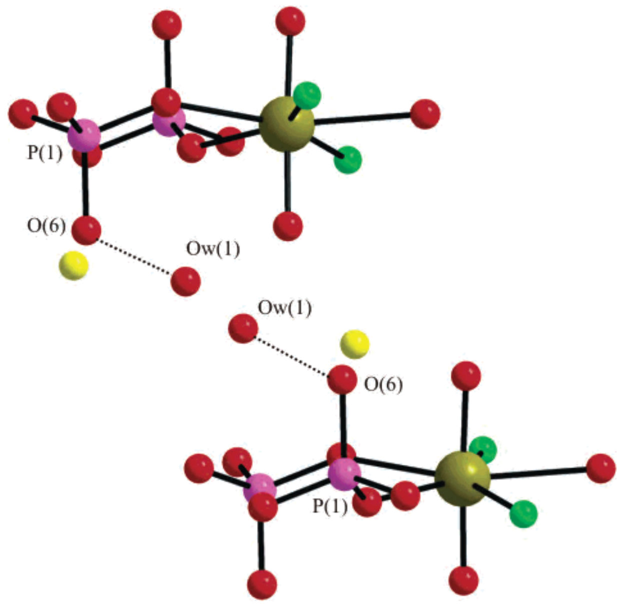

Figure 5. Hydrogen-bonding interactions between the water molecule and hydroxyl group in LUPF-3.

Table 5. IR and Raman Vibrations (cm^{-1}) for LUPF-1, LUPF-2, and LUPF-3

	LUPF-1	LUPF-2	LUPF-3
	IR		
ν_s(U−F)	421	422	412
	452	451	450
	471	472	472
			487
ν_s(U═O)	825	817	821
	840		902
	879	902	
ν_{as}(U═O)	910	921	
ν(P−O)	1029	1029	1026
	1126	1122	1123
δ(P−OH)	1225	1245	1264
δ(O−H)	1635		1612
ν(O−H)	3518		3550
	Raman		
δ(F−U−F)	142	142	139
	187	183	183
	213	219	228
δ(O−U−O)	239	250	256
	267	280	267
ν_{as}(U−F)	340	310	340
			387
ν_s(U−F)	399		
ν_s(U═O)	836	824	833

ment such as acentric dodecahedron or square antiprism, which induces a macroscopic noncentrosymmetric crystal structure.[55] The size of alkali metal cations can also affect the interlayer spacing, which subsequently affects the contact limits of other linkers, structure dimension, and overall centricity.[56,57] Similarly, the alkali metal cations between the layers in LUPF-1, LUPF-2, and LUPF-3 reveal different cation arrangements, which influence the hydrogen-bonding mode and define the centricity for each material. With LUPF-1, to effectively maintain charge neutrality by larger Cs^+ cations, the layers adapt staggered and zigzag environments. By doing so, hydrogen-bonding interactions between the water molecules and hydroxyl groups are possible, which induce LUPF-1 to contain a unique polar axis such as 2_1 along the *c* axis. With LUPF-2, relatively bigger Rb^+ cations drive interlayer arrangement to an eclipsed manner to retain the charge balance, which gives interlayer oxygen hydrogen-bonding interactions between uranyl and phosphate oxygen atoms (See Figure 3). Now, one can clearly find the alignment of asymmetric HPO_4 tetrahedra pointing along the *c* axis, which makes the structure crystallize in noncentrosymmetric space group $Cmc2_1$. Finally, the smaller interlayer spacing in LUPF-3 allows the K^+ cations to interact symmetrically with oxygen atoms in adjacent layers and make the structure centrosymmetric. Powder SHG measurements for the two noncentrosymmetric materials, LUPF-1 and LUPF-2, were performed. The SHG test on pure ungraded samples exhibited an SHG response of about 50% that of the SiO_2 standard for both materials. The observation of low SHG intensity from both of the products is not surprising, because no polarizable cations such as d^0 transition metals or lone-pair cations are incorporated in the materials. However, the SHG signals confirm the acentricity of the space group for both materials.

The vibrational modes of the UO_2F_5 moiety have been well-established.[58,59] The infrared and Raman spectra of the materials revealed U═O and U−F stretches at ca. 820−920 and 140−480 cm^{-1}, respectively. The stretches of P−O are observed around 1030−1120 cm^{-1}. In addition, the deformation of the P−O−H unit for each material was observed around 1250 cm^{-1}, which confirms the presence of the HPO_4 group. Finally, vibrations attributable to H_2O were observed at ca. 1610−1630 and 3500 cm^{-1}. The IR and Raman vibrations and assignments are listed in Table 5. The assignments are consistent with those previously reported.[58−61]

The thermal behaviors of all the reported materials were investigated using thermogravimetric analysis. In each case, a loss of occluded water molecules and/or HF occurred. For LUPF-1, an occluded water molecule is lost between approximately 270 and 300 °C, calculated (experimental): 1.71% (1.64%), and then HF is lost between 370 and 520 °C, calculated (experimental): 5.51% (4.25%). LUPF-2 reveals a weight loss of 4.78% between 230 and 280 °C, which is attributed to the loss of the HF molecule from the material (calculated 4.25%). For LUPF-3, the occluded water molecule is lost between approximately 240 and 300 °C, calculated (experimental): 4.07% (3.92%), and then HF is lost between 370 and 460 °C, calculated (experimental): 8.60% (8.61%). The calcined products for all three reported materials revealed amorphous phases based on the powder XRD measurements.

(55) Bergman, J. G., Jr.; Boyd, G. D.; Ashkin, A.; Kurtz, S. K. *J. Appl. Phys.* **1969**, *70*, 2860.
(56) Sykora, R. E.; Ok, K. M.; Halasyamani, P. S.; Albrecht-Schmitt, T. E. *J. Am. Chem. Soc.* **2002**, *124*, 1951.
(57) Goodey, J.; Ok, K. M.; Broussard, J.; Hofmann, C.; Escobedo, F. V.; Halasyamani, P. S. *J. Solid State Chem*. **2003**, *175*, 3.
(58) Flint, C. D.; Tanner, P. A. *J. Chem. Soc., Faraday Trans. 2* **1981**, *77*, 2339.
(59) Flint, C. D.; Tanner, P. A. *J. Chem. Soc., Faraday Trans. 2* **1984**, *80*, 219.
(60) Bazan, B.; Mesa, J. L.; Pizarro, J. L.; Lezama, L.; Pena, A.; Arriortua, M. I.; Rojo, T. *J. Solid State Chem.* **2006**, *179*, 1459.
(61) Chena, C.; Yi, Z.; Bi, M.; Liu, Y.; Wang, C.; Liu., L.; Zhao, Z.; Pang, W. *J. Solid State Chem.* **2006**, *179*, 1478.

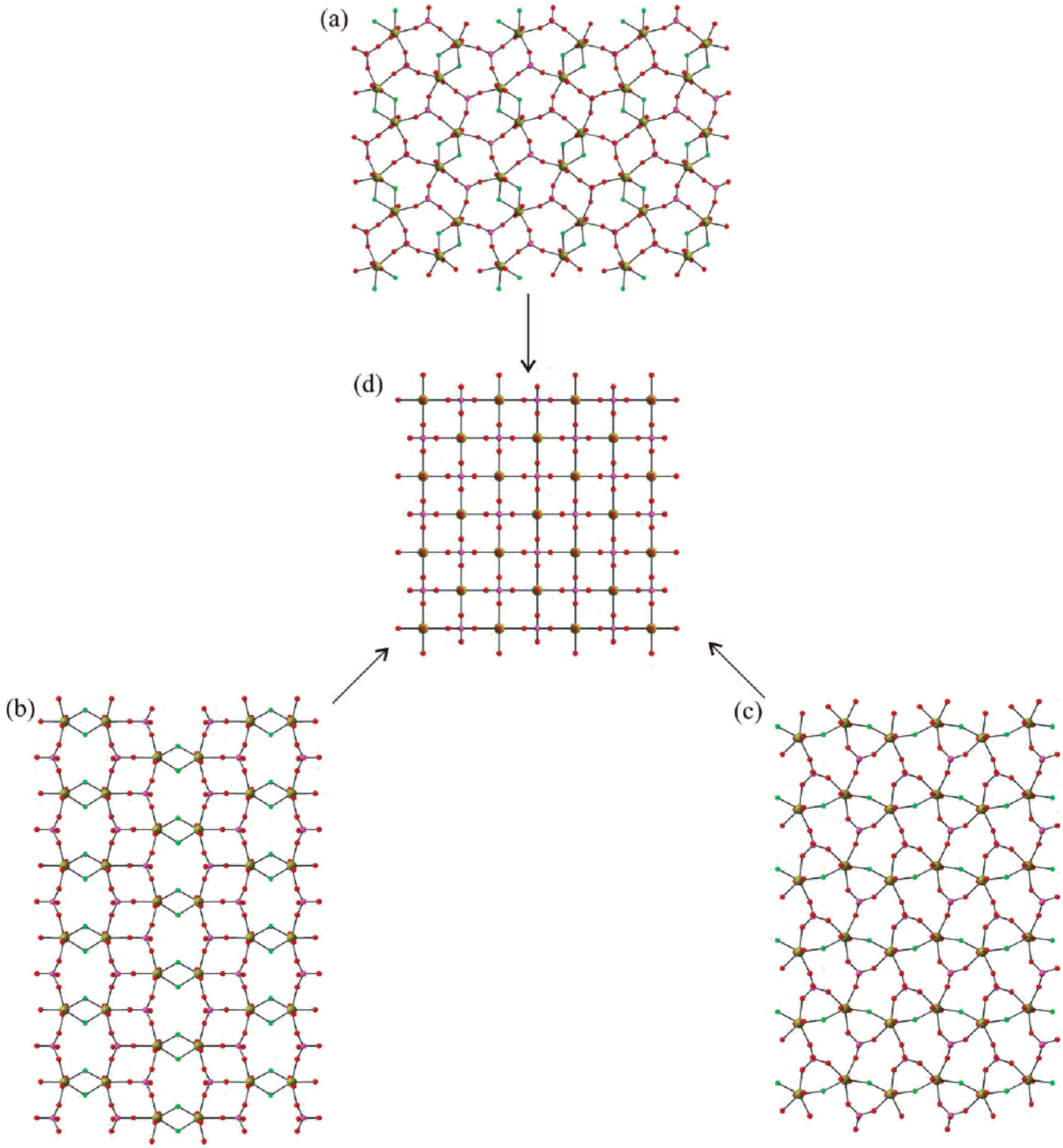

Figure 6. Ball-and-stick representations to show how the structural moieties in each layer transform by the ion-exchange reactions from (a) LUPF-1, (b) LUPF-2, and (c) LUPF-3 to (d) $A(UO_2)(PO_4)\cdot xH_2O$ ($A = Rb^+$, K^+, Na^+, or Li^+; $x = 3$ or 4).

The layered nature of LUPF-1, LUPF-2, and LUPF-3 suggested that the materials may be able to undergo ion-exchange reactions in which the alkali metal cations are replaced by other cationic species. Thus, all three host materials' suspensions were stirred in a ~1 M solution of the appropriate cationic salts for 1 day at room temperature and then an additional 2 days at 50 °C. ICP analyses of the ion-exchanged products revealed that 100% of the Cs^+ cations in LUPF-1 were exchanged for K^+. With LUPF-2, Rb^+ was exchanged for K^+ (96%), Na^+ (42%), and Li^+ (87%) cations. Finally, with LUPF-3, we were able to exchange the K^+ for Rb^+ (100%), Na^+ (43%), and Li^+ (72%) cations (see Figure 6). The powder X-ray diffraction patterns revealed that the exchanged materials are highly crystalline and have very similar XRD patterns. The ion-exchanged materials may be indexed on a tetragonal unit cell. This unit cells as well as the powder X-ray diffraction patterns match well with $A(UO_2)(PO_4)\cdot xH_2O$ (A = Li, Na, K, or Rb; $x = 3$ or 4).[62,63] All of the XRD patterns as well as unit-cell refinements for the ion-exchanged materials are deposited in the Supporting Information. As can be seen in Figure 6,

(62) Weigel, F.; Hoffmann, G. *J. Less-Common Met.* **1976**, *44*, 99.
(63) Chernorukov, N. G.; Karyakin, N. V. *Russ. Chem. Rev. (Engl. Transl.)* **1995**, *64*, 913.

different morphologies of each layer can be easily transformed by ion-exchange reactions in mild conditions. Our experiments demonstrate that the ion exchange of $A(UO_2)F(HPO_4)\cdot xH_2O$ materials not only provide a facile route for the low-temperature synthesis of layered alkali-metal uranium phosphate materials but also suggest how the structural diversity of the uranium layered materials can be tuned with different cations.

Conclusion

In summary, we have reported syntheses, structures, and properties of three new uranium oxide fluorides, LUPF-1, LUPF-2, and LUPF-3. All of the reported materials represent two-dimensional layered structures. The ability of U^{6+} cations to adopt different environments such as $[(UO_2)O_3]_2F_2$ dimers or UO_5F_2 infinite chains, in combination with the tetrahedral moiety of HPO_4 offers various geometries of ring formation within each layer. LUPF-1 and LUPF-2 crystallize in noncentrosymmetric space groups and show weak SHG responses. Of particular interest are the ion-exchange properties for all three materials, which provide a facile route for the low-temperature synthesis of new alkali-metal uranium oxides.

Acknowledgment. We acknowledge Dr. Andrew R. Cowley for crystallographic assistance. We also acknowledge Dr. Christoph Salzmann in obtaining the Raman spectra. K.M.O. and D.O'H. thank the EPSRC for support. J.B. and P.S.H. thank the Robert A. Welch Foundation, the NSF-Career Program (Grant DMR-0092054), and the NSF-Chemical Bonding Center for support.

Supporting Information Available: Powder X-ray diffraction patterns (calculated and experimental) for all the reported materials and powder X-ray diffraction data with refined unit-cell parameters for the ion-exchanged materials are available (PDF). A file of X-ray crystallographic data is also available (CIF). This material is available free of charge via the Internet at http://pubs.acs.org.

IC061420D